

# Single-photon cesium Rydberg excitation spectroscopy by using of 318.6-nm UV laser and room-temperature cesium vapor cell

JIEYING WANG,<sup>1,2</sup> JIANDONG BAI,<sup>1,2</sup> JUN HE,<sup>1,2,3</sup> AND JUNMIN WANG<sup>1,2,3,\*</sup>

<sup>1</sup> State Key Laboratory of Quantum Optics and Quantum Optics Devices, Shanxi University, Tai Yuan 030006, Shan Xi Province, People's Republic of China

<sup>2</sup> Institute of Opto-Electronics, Shanxi University, Tai Yuan 030006, Shan Xi Province, People's Republic of China

<sup>3</sup> Collaborative Innovation Center of Extreme Optics, Shanxi University, Tai Yuan 030006, Shan Xi Province, People's Republic of China

\* [wwjjmm@sxu.edu.cn](mailto:wwjjmm@sxu.edu.cn)

**Abstract:** Single-photon Rydberg excitation spectroscopy of cesium (Cs) atoms is performed in a room-temperature vapor cell. Cs atoms are excited directly from  $6S_{1/2}$  ground state to  $nP_{3/2}$  ( $n = 70 - 100$ ) Rydberg states with a 318.6 nm ultraviolet (UV) laser, and single-photon Rydberg excitation spectra are obtained by transmission enhancement of a probe laser beam resonant to Cs  $6S_{1/2}$  ( $F = 4$ ) -  $6P_{3/2}$  ( $F' = 5$ ) transition as partial population on ( $F = 4$ ) ground state are transferred to Rydberg state. Velocity-selective spectra of Cs  $71P_{3/2}$  Rydberg state are reasonably acquired, and amplitude and linewidth of the spectra influenced by laser intensity have been quantitatively investigated. The energies of Cs  $nP_{3/2}$  ( $n = 70 - 100$ ) Rydberg states are measured, and the quantum defect is obtained by fitting the experimental data. The demodulated spectral signal of single-photon Rydberg excitation spectroscopy is employed to stabilize the UV laser frequency to specific Cs Rydberg transition.

**Key words:** Rydberg states; Spectroscopy, high-resolution; Laser stabilization

## 1. Introduction

Rydberg atoms with principal quantum number  $n \gg 1$  have long been actively investigated. Their huge polarizabilities ( $\sim n^7$ ) give rise to strong dipole-dipole interactions [1], long interaction time [2] and extreme sensitivity to external electric fields [3, 4]. Precision spectroscopy of such state enables demonstrations in metrology [5, 6] and quantum information processing [7-9]. In particular, strong long-range interactions between highly excited Rydberg atoms can lead to Rydberg blockades [10, 11]. The ability to turn the interaction on and off would provide diverse applications for quantum communication [12, 13]. For alkali metal atoms, direct excitation from the ground state to the desired Rydberg states usually requires high-power ultraviolet (UV) laser which is now not commercially available; thus, people commonly prefer a two-photon excitation configuration. However, compare to single-photon Rydberg excitation, two-photon scheme have following disadvantages: atom decoherence due to photon scattering from the lower and upper transitions, and light shift of involved ground state and Rydberg state due to the lower and upper excitation laser beams. Moreover, the selection rules of electrical dipole transition allow only excitation of  $nS$  and  $nD$  Rydberg states in two-photon scheme, and prevent access of  $nP$  Rydberg states. Up to now, studies of single-photon Rydberg excitation are rare, especially in a room-temperature alkali metal vapor cell.

Recently, fiber lasers, fiber amplifiers as well as efficient nonlinear frequency conversion materials have enabled single-photon excitation of Rydberg states. In 2004, Tong *et al* [14] reported single-photon excitation of rubidium (Rb) atoms, and observed the local blockade with field ionization detection in a cold atomic ensemble. While this detection method has high efficiency and discrimination, the detected atoms are removed from the system and cannot be reused. For quantum information applications, nondestructive detection of Rydberg states is necessary. Using direct excitation, Biedermann group [15, 16] recently demonstrated Rydberg

blockade and controlling quantum entanglement between two cesium (Cs) atoms with the loss-detection technique in two close optical dipole traps. For purely optical detection in a room-temperature vapor cell, most laser spectra of Rydberg atoms are two-photon scheme [6, 17, 18]. Therefore, few research involve  $nP$  Rydberg states, especially those with high principle numbers ( $n > 70$ ). In 2009, Thoumany *et al* [19] reported single-photon excitation spectroscopy of Rb  $6P$  state with a 297 nm UV laser in Rb vapor cell.

Here, optically detected single-photon Rydberg excitation spectroscopy of Cs atoms in a room-temperature vapor cell is demonstrated. It is the first observation of velocity-selective spectra of Cs  $6S_{1/2}$  ( $F = 4$ ) -  $nP_{3/2}$  single-photon Rydberg transition with a 318.6 nm UV coupling laser. An 852.3 nm probe laser is used to detect the weak excitation signal. The dependences of the spectral linewidths and amplitudes on the intensities of the coupling and probe lasers are investigated quantitatively. From the Rydberg spectra, energies are obtained for the  $nP_{3/2}$  states, and a quantum defect of 3.56671(42) for  $nP_{3/2}$  states is determined by fitting the experimental data. The demodulated excitation spectrum is employed to lock the UV laser frequency to a specific Rydberg transition.

## 2. Experimental principle and setup

Optical detection of Rydberg excitation is different from that of the first excited state. The low transition probability and the small light-scattering cross sections lead to poor absorption signals. To increase the signal, an alternative detection method is adopted. The direct Rydberg transitions are detected by transmission enhancement of an 852 nm probe laser beam resonant to Cs  $6S_{1/2}$  ( $F = 4$ ) -  $6P_{3/2}$  ( $F' = 5$ ) cycling transition. Fig. 1(a) shows a three-level system interacting with two laser fields composed of the ground state  $6S_{1/2}$  ( $F = 4$ ), an excited state  $6P_{3/2}$  ( $F' = 5$ ) or  $6P_{3/2}$  ( $F' = 4$ ), and a Rydberg state  $nP_{3/2}$ . Because the lifetime of  $nP_{3/2}$  ( $n = 70 - 100$ ) Rydberg states is longer than 100  $\mu s$  [2], some atoms populated on  $6S_{1/2}$  ( $F = 4$ ) state will be transferred to the long-lifetime Rydberg state as the frequency of 318.6 nm laser is scanned across it. When the population on  $6S_{1/2}$  ( $F = 4$ ) state decreases, the transmission of the 852.3 nm probe laser will be enhanced.

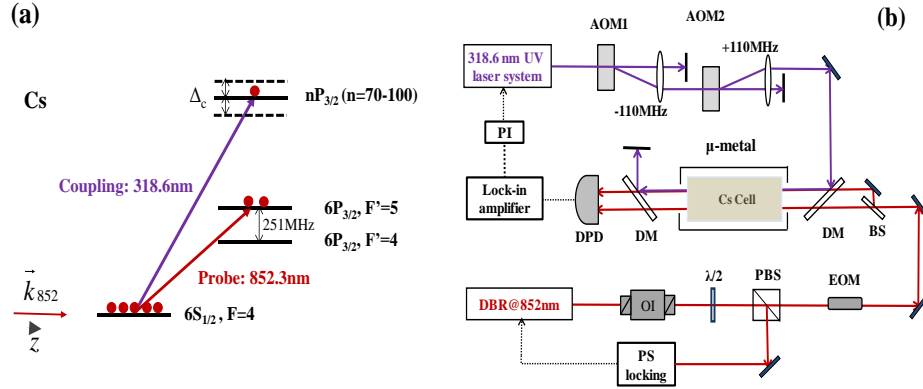


Fig. 1. (a) Relevant hyperfine levels for Cs atomic single-photon Rydberg excitation. The 852.3 nm probe laser is resonant with  $6S_{1/2}$  ( $F = 4$ ) -  $6P_{3/2}$  ( $F' = 5$ ), and the 318.6 nm coupling laser is scanned through the resonances from  $6S_{1/2}$  ( $F=4$ ) to  $nP_{3/2}$  Rydberg states. (b) Schematic of the experimental arrangement of a 318.6 nm coupling laser co-propagating with an 852.3 nm probe laser in a 10-cm-long Cs vapor cell. DBR: distributed-Bragg-reflector diode laser; OI: optical isolator;  $\lambda/2$ : half-wave plate; PBS: polarization beam splitter cube; DM: dichroic mirror; BS: 50:50 beam splitter; AOM: acousto-optic modulator; PI: proportion and integration amplifier; EOM: electro-optic modulator; DPD: differential photodiode; PS: polarization spectroscopy.

For a three-level scheme, the observed spectroscopy in a room-temperature vapor cell is usually a velocity-dependent spectrum [20, 21]. Taking into account Doppler effect, the frequency of probe laser for different velocity-groups atoms is:

$$v = v_0 \left(1 + \frac{v_z}{c}\right) = v_0 + \Delta_p \quad (1)$$

where  $v_0$  is the reference frequency;  $c$  is the speed of light in vacuum;  $v_z$  is the atomic velocity component along the direction of the probe beam;  $\Delta_p = v_z/c$  is the detuning of probe laser. Reasonably Cs  $6S_{1/2}$  ( $F = 4$ ) -  $6P_{3/2}$  ( $F' = 5$ ) cycling transition is set as the reference frequency. For atoms with velocity of  $v_z = 0$ , the detuning of the probe laser is  $\Delta_p = 0$ . For atoms with velocity groups of  $v_z = -213.94$  m/s,  $\Delta_p$  is  $-251$  MHz, which will result in a resonance with hyperfine states of ( $F = 4$ ) - ( $F' = 4$ ). In view of the wavelength mismatch, if the frequency of the 318.6 nm laser matches these atomic groups to the levels of  $nP_{3/2}$ , the Rydberg excitation signal can be detected. The corresponding detuning of the copropagating coupling laser  $\Delta_c$  can be given as  $\Delta_c = \Delta_p (\lambda_p / \lambda_c)$ , where  $\lambda_p$ ,  $\lambda_c$  are the wavelengths of the probe and coupling lasers, respectively.

A schematic of the experimental setup is shown in Fig. 1(b). The high-power 318.6 nm UV coupling laser is generated by cavity-enhanced second harmonic generation following sum-frequency generation of two infrared lasers at 1560.5 nm and 1076.9 nm. As discussed previously,  $\sim 2$  W tunable UV laser was obtained [22, 23]. The frequency of the coupling laser is tuned to Rydberg transition  $6S_{1/2}$  ( $F = 4$ ) -  $nP_{3/2}$  ( $n = 70 - 100$ ) over the range of 318.5 - 318.7 nm. The weak probe laser is produced by an 852 nm distributed-Bragg-reflector (DBR) diode laser, and its frequency is locked to Cs  $6S_{1/2}$  ( $F = 4$ ) -  $6P_{3/2}$  ( $F' = 5$ ) cycling transition using polarization spectroscopy (PS). A waveguide-type electro-optic modulator (EOM) (Photline, NIR-MX800) at 852 nm is used to calibrate the spectral interval. The coupling and probe lasers are collimated to diameters of  $\sim 1.6$  and  $\sim 1.3$  mm ( $1/e^2$ ), respectively, and both are linearly polarized. The probe laser is split into two beams of equal power before entering a 10-cm-long fused-quartz Cs cell, and one beam is superposed with the 318.6 nm coupling laser using a dichroic mirror. The Cs vapor cell is placed in a  $\mu$ -metal-shielded enclosure to reduce residual magnetic fields. The transmission of the probe laser is detected with a differential photodiode (DPD) (New Focus, 2107) after the laser passed through another dichroic mirror that is a high reflectivity mirror for 318.6 nm. When the UV laser is scanned through a specific single-photon Rydberg transition, some atoms are transferred to Rydberg state, enhancing the transmission of the probe laser that is overlapped with the coupling laser (Fig. 2(a)). The frequency of the coupling laser is calibrated by a wavelength meter (Toptica-Amstrong, HighFinesse WS-7). The detected signal is demodulated with a lock-in amplifier (SRS, SR830), creating an error signal. The error signal is fed back to the piezoelectric transducer of the 1076.9 nm fiber laser to compensate the frequency deviation using a feedback proportion and integration amplifier (PI) (SRS, SIM960). The lock-in demodulation is enabled by UV laser frequency modulation with an acousto-optic modulator (AOM2) (Gooch & Housego, I-M110-3C10BB-3-GH27), and the modulation signal from the lock-in amplifier is added to the 110 MHz central frequency. Two AOMs with opposite frequency shift are used to compensate the frequency shift from a single AOM, this ensure that the UV laser frequency is locked to a Rydberg transition.

### 3. Observation of velocity-selective spectra of Cs $6S_{1/2}$ - $71P_{3/2}$ Rydberg excitation

Keeping the 852.3 nm probe laser locked to Cs  $6S_{1/2}$  ( $F = 4$ ) -  $6P_{3/2}$  ( $F' = 5$ ) cycling transition and the 318.6 nm coupling laser scanned through the resonances of  $6S_{1/2}$  ( $F = 4$ ) to  $71P_{3/2}$  Rydberg states, the observed single-photon Rydberg spectra is shown in Fig. 2(a) when they copropagate in the Cs cell. A small transmission peak appears when the UV laser frequency is blue-detuned to the resonance frequency of  $71P_{3/2}$  state. Analysis revealed that the excitation signal derive from different velocity groups ( $v_z = 0$  and  $v_z = 213.9$  m/s) of the atoms, and the small peak is attributed to Cs  $6S_{1/2}$  ( $F = 4$ ) -  $6P_{3/2}$  ( $F' = 4$ ) hyperfine transition.

A radio-frequency modulation combined with the velocity-selective spectroscopy is used to calibrate the peak splitting. The spectral resolution is limited only by the signal linewidth.

Fig. 2(b) is a sideband calibration result with radio-frequency modulation frequency of 70 MHz for 852.3 nm probe laser. In view of the wavelength mismatch of  $\lambda_p / \lambda_c \approx 2.675$ , the observed hyperfine interval turn into  $\sim 187$  MHz. While the RF modulation frequency of EOM is 251 MHz, the +1-order sideband of the main peak is superposed on the small peak. Using  $\Delta_c = \Delta_p$  ( $\lambda_p / \lambda_c$ ), the observed hyperfine interval of the spectra becomes  $\sim 671$  MHz.

To further verify that the excitation signal arise from the hyperfine splitting rather than fine splitting of nP Rydberg states as [19], the interval between the two peaks is measured using a wavelength meter as the principal number n is varied from 70 to 100. Result shows that the UV detuning is a constant of  $\sim 670$  MHz, and no decrease with increasing principal number. Furthermore, the direct excitation oscillator strength of Cs nP<sub>1/2</sub> state is nearly four orders of magnitude smaller than that of Cs nP<sub>3/2</sub> state [15], and can't be observed here. The main transmission peak of the copropagation scheme is used for the following experiment.

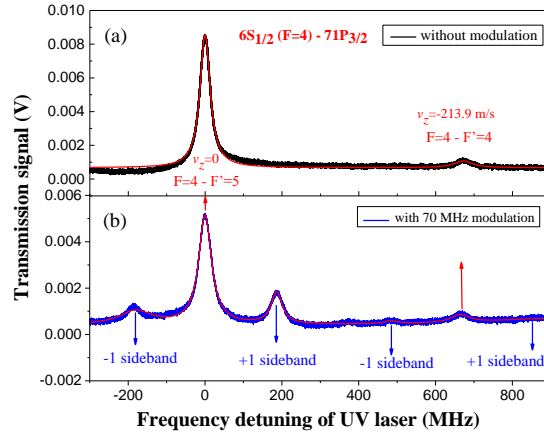


Fig. 2. (a) The excitation spectra of  $6S_{1/2}(F=4) - 71P_{3/2}$  Rydberg transition in a Cs vapor cell when the 852.3 nm probe laser is locked to Cs  $6S_{1/2}(F=4) - 6P_{3/2}(F'=5)$  cycling transition. The intensities of coupling and probe lasers are  $\sim 1.99 \times 10^4$  mW/cm<sup>2</sup> and  $\sim 3.01$  mW/cm<sup>2</sup>, respectively. (b) Sideband calibration result with a radio-frequency modulation of 70 MHz for 852.3 nm probe laser, considering the Doppler factor of  $\lambda_p / \lambda_c \approx 2.675$ , the observed hyperfine interval becomes  $\sim 187$  MHz. Red curve is a multi-peak Lorentz fitting.

### 3.1 Linewidths and amplitudes of Rydberg spectra versus laser intensity

The probability of single-photon Rydberg transition for high n is quite small relative to that of the first excited state. For example, the oscillator strength for Cs  $6S_{1/2} - 84P_{3/2}$  transition is  $6 \times 10^{-8}$  [15], while it is 0.7164 for Cs  $6S_{1/2} - 6P_{3/2}$  transition. Thus, improving the signal-to-noise ratio and simultaneously suppressing spectral broadening of the weak excitation signal is critical for precision spectroscopy.

To study the influence of the coupling and probe laser's intensities on the single-photon spectra, the signal is measured as a function of probe laser intensity  $I_p$  for various coupling laser intensities  $I_c$ . An EOM with a 70-MHz modulation frequency, corresponding to a UV detuning of  $\sim 187$  MHz, is used to calibrate the linewidth of the main peak in the Rydberg spectra. Results show that while the amplitude of the peak increase significantly with both coupling and probe laser intensities (Fig. 3(a)), the spectral signal broadening becomes no longer negligible (Fig. 3(b)). The linewidth increased linearly with probe laser intensity and much less with coupling laser intensity. When the intensity of the probe laser exceeded  $\sim 45$  mW/cm<sup>2</sup>, the peak begins to undergo Autler-Townes splitting. The narrowest linewidth is 24 MHz for  $I_c \sim 0.25 \times 10^4$  mW/cm<sup>2</sup> and  $I_p \sim 1.9$  mW/cm<sup>2</sup>. Considering the Doppler mismatch, the power broadening from probe laser is  $\sim 21$  MHz, which is obtained from  $\gamma_p = \gamma (1 + I_p / I_c)^{1/2}$ , where  $\gamma = 5.2$  MHz is the

natural linewidth and  $I_s = 1.12 \text{ mW/cm}^2$  is the saturation intensity of Cs D2 line. Extrapolation to  $I_p = 0$  yields 16(2) MHz. These results contain contributions from the natural linewidth of  $\sim 14 \text{ MHz}$  ( $\sim 2.675 \times 5.2 \text{ MHz}$ ), transit-time broadening of  $\sim 450 \text{ kHz}$  ( $\sim 2.675 \times 168 \text{ kHz}$ ), collision broadening, and possibly power broadening from the coupling laser. Broadening mechanism of Rydberg states in different pressure was qualitatively investigated [24], and the observed narrowest linewidth was 10 MHz. Spectral broadening of Rydberg resonance lines resulting from high-power excitation laser in cold atoms was also observed [25]. Narrow linewidth with high signal-to-noise ratio is important for stabilizing the laser frequency to specific Rydberg transition and for precision spectroscopy.

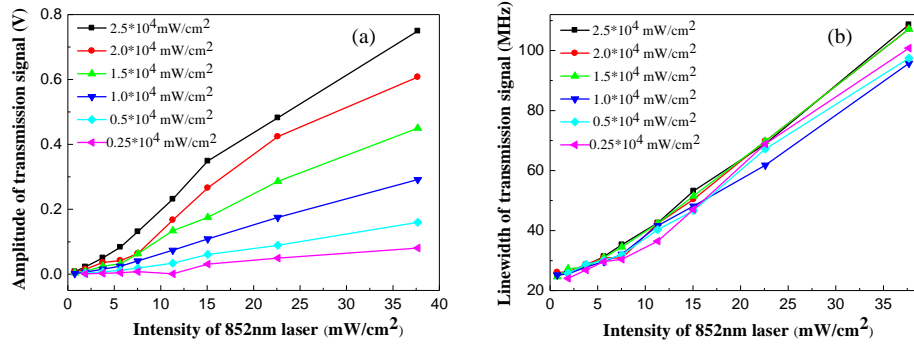


Fig. 3. Amplitudes (a) and linewidths (b) of Cs  $6S_{1/2}$  ( $F = 4$ ) -  $71P_{3/2}$  single-photon Rydberg transmission spectra as a function of probe laser intensity for different coupling laser intensities. The narrowest linewidth is 24 MHz with  $I_c \sim 0.25 \times 10^4 \text{ mW/cm}^2$  and  $I_p \sim 1.9 \text{ mW/cm}^2$ .

### 3.2 Measurement of quantum defect for Cs $nP_{3/2}$ states

Quantum defect is an important parameter for Rydberg atoms. Because Cs atoms have a big  $\text{Cs}^+$  core, quantum defects for the lower orbital angular momentum states (S, P, D) are relatively large. Energy levels of Cs atoms are predicted with high precision by quantum defect theory, where energies of the  $nP$  states can be represented by the modified Ritz formula [2]:

$$E(n, l) = E_\infty - \frac{R_{\text{Cs}}}{(n - \delta_{n,l})^2} - E_f \quad (2)$$

where  $E(n, l)$  is the energy of the level with principal quantum number  $n$  and angular quantum number  $l$ ,  $E_\infty = 31406.46766 \text{ cm}^{-1}$  is the ionization threshold energy,  $R_{\text{Cs}}$  is the Cs Rydberg constant of  $109736.86274 \text{ cm}^{-1}$ ,  $E_f = 4.0217764 \text{ GHz}$  is the hyperfine frequency shift of the Cs  $6S_{1/2}$  ( $F = 4$ ) hyperfine component from the  $6S_{1/2}$  ground state. The parameter  $\delta_{n,l}$  is the quantum defect given as follows [2]:

$$\delta_{n,l} = \delta_0 + \frac{\delta_1}{(n - \delta_0)^2} + \frac{\delta_2}{(n - \delta_0)^4} + \dots \quad (3)$$

For  $n \geq 70$ , the quantum defect can be treated as a constant for the same angular momentum states as the higher order terms of  $\delta_{n,l}$  are small and can be neglected [2].

The energy data of the Cs  $nP_{3/2}$  states ( $n = 70 - 100$ ) is plotted in Fig. 4, where the measurement range of principle number  $n$  is mainly limited by the tuning range of our UV laser system. The measured energy data for Rydberg states (dots) are fitted with Eq.2 (solid line), yielding a quantum defect of 3.56671(42) for  $nP_{3/2}$  states. The accuracy is limited by the wavelength meter and the linewidth of the 852 nm DBR laser.

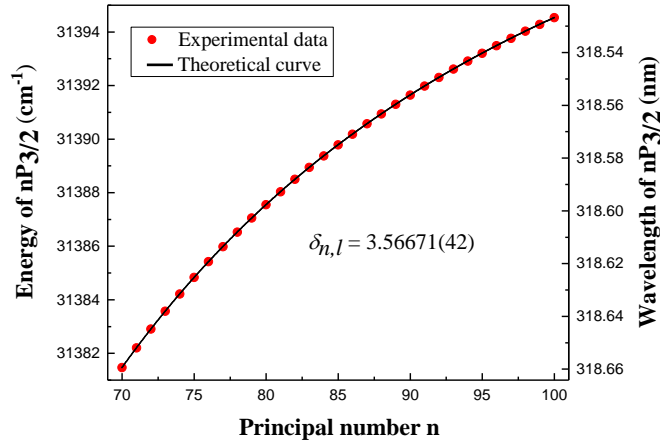


Fig. 4. Energies of Cs  $nP_{3/2}$  Rydberg states ( $n = 70 - 100$ ). The dots are experimental data, and the solid line is the fitting curve. The quantum defect of Cs  $nP_{3/2}$  states is  $3.56671(42)$ , where the error is statistical error.

#### 4. UV laser frequency stabilization with single-photon Cs Rydberg spectra

After optimizing the linewidth and signal-to-noise ratio, we reasonably choose Rydberg spectrum of Cs  $6S_{1/2}$  ( $F = 4$ ) -  $71P_{3/2}$  transition with 27.3 MHz linewidth ( $I_c \sim 1.5 \times 10^4$  mW/cm<sup>2</sup> and  $I_p \sim 1.9$  mW/cm<sup>2</sup>) as the reference frequency to stabilize the UV laser, as shown in the upper part of Fig. 5(a). Here the probe laser is frequency modulated at 17 kHz by AOM2. A dispersive signal is obtained with the lock-in amplifier (the lower part of Fig. 5(a)), which is fed back to the piezoelectric transducer of the 1076.9 nm fiber laser to compensate the frequency deviation using a feedback PI controller. The estimated bandwidth of the servo loop is  $\sim 10$  kHz, which is limited by the demodulation time (300  $\mu$ s) of the lock-in amplifier. Using the main peak of the Rydberg spectra as the reference frequency, the UV laser frequency is locked to the zero-crossing point.

The Allan deviation of a locking laser system should be measured by the optical frequency comb technique or the beat note of two identical laser systems, which can accurately reveal the laser frequency stability. Unfortunately, the commercial UV optical frequency combs are very scarce and we don't have another same UV laser system. Assuming the single-photon Rydberg excitation spectrum is absolutely stable, and the reference point is not time-varying, the relative Allan deviation can be used to characterize the frequency stability of the locking system. Fig. 5(b) shows relative Allan deviation of the UV laser, and the relative frequency stability is estimated from the slope of the zero-crossing point in the error signal. Typical relative frequency stability (fluctuation) is  $\sim 3.2 \times 10^{-10}$  ( $\sim 300$  kHz) for the interrogation time of 1 s, and it is  $\sim 1.3 \times 10^{-11}$  ( $\sim 12$  kHz) for the interrogation time of 56 s. It should be emphasized that the Allan deviation is originated from the error signal, which is not an absolute frequency standard; thus, it only represents a lower limit of the frequency instability. However, 300 kHz is still a considerable improvement over the large frequency fluctuation of free running (several megahertz over 1 s). Hence, the frequency locking technique is effective to compensate the long-term frequency drift of the UV laser. The frequency stability is sufficient to perform the Cs  $6S_{1/2}$  to  $nP_{3/2}$  ( $n = 70-100$ ) single-photon Rydberg excitation.

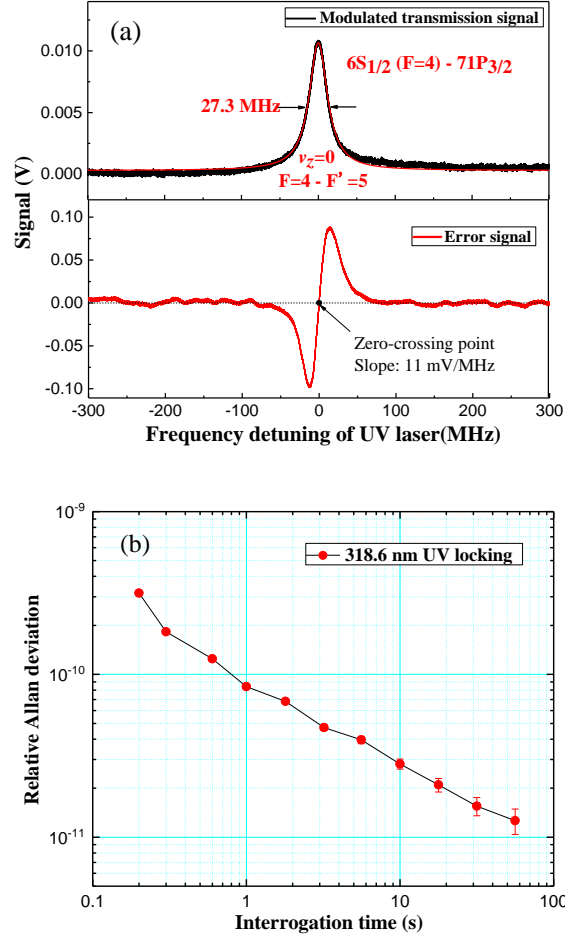


Fig. 5. (a) The transmitted signal of the frequency-modulated Rydberg spectra with  $I_c \sim 1.5 \times 10^4$  mW/cm<sup>2</sup> and  $I_p \sim 1.9$  mW/cm<sup>2</sup> and the corresponding error signal from the lock-in amplifier with a modulation frequency and demodulation time of 17 kHz and 300  $\mu$ s, respectively. (b) Relative Allan standard deviation plots show the relative frequency instability of the 318.6 nm UV laser (dots) while the coupling laser keep locked.

## 5. Summary

We have performed a single-photon Rydberg excitation spectroscopy of Cs atoms in a room-temperature vapor cell using an optical detection method. The velocity-selective spectra of Cs  $6S_{1/2}$  ( $F = 4$ ) -  $nP_{3/2}$  ( $n = 70 - 100$ ) transitions are consistent with theoretical analysis of the Doppler mismatch. The dependence of the spectral linewidths and amplitudes on the coupling and probe laser intensities is quantitatively investigated. From Rydberg spectra, energy data of Cs  $nP_{3/2}$  ( $n = 70 - 100$ ) Rydberg states is obtained, and this yields the quantum defect of 3.56671(42) by a fitting of Ritz formula. The measurement accuracy is mainly limited to the wavlengthmeter's accuracy and the linewidth of the 852 nm DBR laser which is used in our experiment. After optimization of the spectral parameters, the error signal, obtained by demodulating the signal, is used to lock the UV laser frequency to a specific Rydberg transition. The experimental results reveals the ability to stabilize the UV laser frequency to one of Cs  $6S_{1/2}$  -  $nP_{3/2}$  ( $n = 70 - 100$ ) Rydberg transitions. Investigation of the high precision single-photon Rydberg spectroscopy in room-temperature Cs atoms should greatly impact and improve the



excitation and detection techniques, especially for studying nP states' energy structure of Rydberg atoms and the interaction between Rydberg atoms.

## Funding

This work is supported by the National Natural Science Foundation of China (NSFC Grant Nos. 61475091 and 61227902), and by the National Key Research and Development Program of China (2017YFA0304502).

## References and links

1. M. Saffman, T. G. Walker, and K. Mølmer, "Quantum information with Rydberg atoms," *Rev. Mod. Phys.* **82**(3), 2313-2363 (2010).
2. T. F. Gallagher, *Rydberg Atoms* (Cambridge University, 1994).
3. M. L. Zimmerman, M. G. Littman, M. M. Kash, and D. Kleppner, "Stark structure of the Rydberg states of alkali-metal atoms," *Phys. Rev. A* **20**(6), 2251-2275 (1979).
4. J. A. Sedlacek, A. Schwettmann, H. Kübler, and J. P. Shaffer, "Atom-based vector microwave electrometry using rubidium Rydberg atoms in a vapor cell," *Phys. Rev. Lett.* **111**(6), 063001 (2013).
5. J. D. Carter, O. Cherry, and J. D. D. Martin, "Electric-field sensing near the surface microstructure of an atom chip using cold Rydberg atoms," *Phys. Rev. A* **86**(5), 053401 (2012).
6. J. A. Sedlacek, A. Schwettmann, H. Kübler, R. Löw, T. Pfau, and J. P. Shaffer, "Microwave electrometry with Rydberg atoms in a vapor cell using bright atomic resonances," *Nature Phys.* **8**(11), 819-824 (2012).
7. B. Zhao, M. Müller, K. Hammerer, P. Zoller, "Efficient quantum repeater based on deterministic Rydberg gates," *Phys. Rev. A* **81**(5), 052329 (2010).
8. T. Wilk, A. Gaëtan, C. Evellin, J. Wolters, Y. Miroshnychenko, P. Grangier, A. Browaeys, "Entanglement of two individual neutral atoms using Rydberg blockade," *Phys. Rev. Lett.* **104**(1), 010502 (2015).
9. L. Isenhower, E. Urban, X. L. Zhang, A. T. Gill, T. Henage, T. A. Johnson, T. G. Walker, M. Saffman, "Demonstration of a neutral atom controlled-NOT quantum gate," *Phys. Rev. Lett.* **104**(1), 010503 (2010).
10. E. Urban, T. A. Johnson, T. Henage, L. Isenhower, D. D. Yavuz, T. G. Walker and M. Saffman, "Observation of Rydberg blockade between two atoms," *Nature Phys.* **5**(5), 110-114 (2009).
11. A. Gaëtan, Y. Miroshnychenko, T. Wilk, A. Chotia, M. Viteau, D. Comparat, P. Pillet, A. Browaeys, and P. Grangier, "Observation of collective excitation of two individual atoms in the Rydberg blockade regime," *Nature Phys.* **5**(5), 115-118 (2009).
12. Y. O. Dudin and A. Kuzmich, "Strongly Interacting Rydberg excitations of a cold atomic gas," *Science* **336**(6083), 887-889 (2012).
13. T. Keating, K. Goyal, Y. Y. Jau, G. W. Biedermann, A. J. Landahl, and I. H. Deutsch, "Adiabatic quantum computation with Rydberg-dressed atoms," *Phys. Rev. A* **87**(5), 052314 (2013).
14. D. Tong, S. M. Farooqi, J. Stanojevic, S. Krishnan, Y. P. Zhang, R. Côté, E. E. Eyler, and P. L. Gould, "Local blockade of Rydberg excitation in an ultra-cold gas," *Phys. Rev. Lett.* **93**(6), 063001 (2004).
15. A. M. Hankin, Y. Y. Jau, L. P. Parazzoli, C. W. Chou, D. J. Armstrong, A. J. Landahl, and G. W. Biedermann, "Two-atom Rydberg blockade using direct 6S to nP excitation," *Phys. Rev. A* **89**(3), 033416 (2014).
16. Y. Y. Jau, A. M. Hankin, T. Keating, I. H. Deutsch, and G. W. Biedermann, "Entangling atomic spins with a Rydberg-dressed spin-flip blockade," *Nature Phys.* **12**(1), 71-74 (2016).
17. S. X. Bao, H. Zhang, J. Zhou, L. J. Zhang, J. M. Zhao, L. T. Xiao, and S. T. Jia, "Polarization spectra of Zeeman sublevels in Rydberg electromagnetically induced transparency," *Phys. Rev. A* **94**(4), 043822 (2016).
18. A. K. Mohapatra, T. R. Jackson, and C. S. Adams, "Coherent optical detection of highly excited Rydberg states using electromagnetically induced transparency," *Phys. Rev. Lett.* **98**(11), 113003 (2007).
19. P. Thoumany, T. Hänsch, G. Stania, L. Urbonas, and T. Becker, "Optical spectroscopy of rubidium Rydberg atoms with a 297 nm frequency-doubled dye laser," *Opt. Lett.* **34**(11), 1621-1623 (2009).
20. Y. C. Jiao, X. X. Han, Z. W. Yang, J. K. Li, G. Raithel, J. M. Zhao, and S. T. Jia, "Spectroscopy of cesium Rydberg atoms in strong radio-frequency fields," *Phys. Rev. A* **94**(2), 023832 (2016).
21. Y. H. Wang, H. J. Yang, Z. J. Du, T. C. Zhang, and J. M. Wang, "Autler-Townes doublet in novel sub-Doppler spectra with cesium vapor cell," *Chin. Phys. B* **15**(1), 138-142 (2006).
22. J. Y. Wang, J. D. Bai, J. He, and J. M. Wang, "Realization and characterization of single-frequency tunable 637.2 nm high-power laser," *Opt. Commun.* **370**, 150-155 (2016).
23. J. Y. Wang, J. D. Bai, J. He, and J. M. Wang, "Development and characterization of a 2.2 W narrow-linewidth 318.6-nm ultraviolet laser," *J. Opt. Soc. Am. B* **33**(10), 2020-2025 (2016).
24. B. P. Stoicheff and E. Weinberger, "Frequency shifts, line broadenings, and phase-interference effects in Rb + Rb collisions, measured by Doppler-free two-photon spectroscopy," *Phys. Rev. Lett.* **44**(11), 733-736 (1980).
25. K. Singer, M. R. Lamour, T. Amthor, L. G. Marcassa, and M. Weidemüller, "Suppression of excitation and spectral broadening induced by interactions in a cold gas of Rydberg atoms," *Phys. Rev. Lett.* **93**(16), 163001 (2004).